NISTIR 6654

Thermodynamic Data to Support High-Temperature Syngas Quench Design: Vapor Liquid Equilibrium Calculations

Allan H. Harvey

National Institute of
Standards and Technology
U.S. Department of Commerce

Thermodynamic Data to Support High-Temperature Syngas Quench Design: Vapor-Liquid Equilibrium Calculations

Allan H. Harvey

Physical and Chemical Properties Division
National Institute of Standards and Technology
325 Broadway
Boulder, Colorado 80305

January 2008

U.S. Department of Commerce
Carlos M. Gutierrez, Secretary

National Institute of Standards and Technology
James M. Turner, Acting Director

ABSTRACT

A procedure has been developed, based on a dilute-solution model of the liquid phase and the rigorous virial expansion for the vapor phase, for modeling the vapor-liquid equilibrium between water and a synthesis gas consisting primarily of H_2, CO, and CO_2. Calculations of the vapor-liquid equilibrium have been performed at temperatures and pressures typical for a quench step in an IGCC power plant. The uncertainty in the calculated vapor-phase mole fraction of water is less than 0.01, and is due primarily to the omission of higher-order terms in the virial expansion.

Other thermodynamic calculation methods were examined and compared to the more rigorous calculations. The ideal-gas assumption for the vapor phase seriously underestimates (by about 0.09 mole fraction at typical conditions) the water content of the equilibrium vapor. The Peng-Robinson equation performs much better, producing vapor-phase mole fractions of water that differ from the more rigorous results by amounts similar to the uncertainty in the virial approach.

This work was performed for the Program for Technology Innovation of the Electric Power Research Institute (EPRI). A version of this report with additional process-related comments from the sponsor perspective is being published separately as an EPRI Report.

1 **INTRODUCTION 1-1**
Background 1-1
Problem Definition 1-1
Approach 1-2

2 **RESULTS 2-1**
Baseline Case Results 2-1
Effects of Temperature and Pressure 2-1
Estimation of Uncertainties 2-3
Uncertainty from Liquid Fugacity Model 2-3
Uncertainty from Second Virial Coefficients 2-3
Uncertainty from Higher Virial Coefficients 2-4
Effect of Gas Composition 2-4
Liquid-Phase Composition 2-5

3 **DISCUSSION 3-1**
Main Results 3-1
Note on “Adiabatic” Flash Calculations 3-1
Possible Enhancements 3-2

A **VAPOR-LIQUID FLASH CALCULATIONS A-1**
Definition of Problem A-1
Description of Algorithm A-1

B **LIQUID-PHASE FUGACITY MODEL B-1**
Fugacity of Gaseous Solutes B-1
Fugacity of Liquid Water B-3
Impact on Calculations B-4

C **VAPOR-PHASE FUGACITY MODEL C-1**
Calculation from Virial Coefficients C-1
B(T) Data for Pure Components C-2
B(T) Data for Aqueous Binaries C-3
B(T) Data for Nonaqueous Binaries C-4
Supplementary Calculation with Peng-Robinson Equation of State C-7

D **REFERENCES D-1**

LIST OF FIGURES

Figure 2-1 Effect of Temperature on Equilibrium Mole Fraction of Water in Vapor at 4.5 MPa 2-2

Figure 2-2 Effect of Pressure on Equilibrium Mole Fraction of Water in Vapor at 495 K 2-2

LIST OF TABLES

Table 1-1 Baseline Composition of Synthesis Gas 1-1

Table 2-1 Equilibrium Liquid (x_i) and Vapor (y_i) Mole Fractions Calculated for the Baseline Case, with Vapor Fugacities Computed by the Ideal-Gas (IG), Virial (Vir), and Peng-Robinson (PR) Methods 2-1

Table 2-2 Effect on Water Content in Vapor of Perturbing Second Virial Coefficient Upward by its (k=2) Uncertainty 2-4

Table B-1 Parameters for Eq. (B4), along with Maximum and Minimum Temperatures of Data Used for the Correlation B-2

Table B-2 Parameters for Eq. (B7). (last column is b_i for all solutes except CO_2, where it is b_i') B-3

Table C-1 Parameters for Eq. (C4) for $B(T)$ of Ar, N_2, CO, CO_2, and CH_4 .... C-3

Table C-2 Critical Parameters and Acentric Factor for Substances Considered in this Work C-3

Table C-3 Parameters for Eq. (C8) for $B_{ij}(T)$ for H_2O with Various Gases C-4

Table C-4 Binary Parameters k_{ij} for Eq. (C15) for Pairs of Nonaqueous Gases C-6

1

INTRODUCTION

Background

The purpose of this work is to provide data relevant to the design of Integrated Gasification Combined Cycle (IGCC) power plants. In some proposed designs, a hot synthesis gas, consisting mostly of H_2, CO, and CO_2, is quenched with water. The amount of water in the resulting gas is a significant factor in the economics of the cycle. Previous efforts to model this step, using a variety of thermodynamic models, have come up with significantly different results. This project was undertaken to perform calculations with a rigorous thermodynamic model in order to provide reliable data for the water vapor content, with reasonable estimates of uncertainties.

Problem Definition

The calculations performed consist of the computation of thermodynamic equilibrium between vapor and liquid (vapor-liquid equilibrium, or VLE). This equilibration takes place at a specified temperature T and absolute pressure p. Based on input from the sponsor, a "baseline" case was defined at a temperature of 495 K (approximately 431 °F) and a pressure of 4.5 MPa (approximately 650 psia).

The "baseline" composition for the dry gas was also taken from sponsor input and is shown in Table 1-1. Other, trace components in the gas phase may exist (such as H_2S, NH_3, and CH_4), but they are outside the scope of this project. While the main result of interest (mole fraction of water in equilibrium vapor) is not very sensitive to the total amount of water in the system, for consistency all calculations assumed five times as many moles of water as moles of dry gas.

Table 1-1
Baseline Composition of Synthesis Gas

Gas	Mole Fraction
Ar	0.01
H_2	0.39
N_2	0.01
CO	0.41
CO_2	0.18

Approach

In order to solve the VLE problem, the fugacity of each component in the liquid phase is equated with its fugacity in the vapor phase under the constraint of fixed T and p. In the terminology of chemical engineering, this is known as a "flash" calculation. The computational algorithm for solving the flash problem is described in Appendix A. This algorithm requires a model for the liquid-phase and vapor-phase fugacities of each component as a function of temperature, pressure, and composition.

For modeling the fugacities in the liquid phase at these moderate pressures, where the solubility of the gases in water is small, it is sufficient to invoke the dilute-solution approximation known as Henry's Law. This primarily requires knowing the Henry's constant for each gas in water as a function of temperature. Additional data on the partial molar volumes of gases in solution provide a small correction for the effect of pressure on the fugacity. The liquid-phase fugacity model used in this work is completely documented in Appendix B.

The most important factor in determining the water content of the equilibrium vapor is the vapor-phase fugacity model. At the conditions of interest, an ideal-gas assumption (common in many engineering calculations) would seriously overestimate the fugacity of water, leading to an underestimation of the equilibrium water mole fraction. The equation-of-state approaches commonly used in engineering thermodynamics are designed primarily for hydrocarbon mixtures, so they cannot be expected to be reliable for mixtures of water with nonpolar gases as encountered in this work.

Our approach here is to model the vapor-phase fugacities by the virial expansion, which is a rigorous series of corrections to the ideal-gas law. At the moderate pressures of interest here, the second virial coefficient (first correction to the ideal gas) provides sufficient accuracy. Therefore, if reliable values of the second virial coefficients among all components in the mixture can be obtained, accurate values of the vapor-phase fugacities can be obtained. Appendix C documents the second-virial-coefficient data used in this work, and their use in fugacity calculations.

For purposes of comparison, we also performed vapor-phase fugacity calculations with the ideal-gas model, and with a common engineering equation of state model (the Peng-Robinson equation, applied only to the vapor phase). These models are also described in Appendix C.

2
RESULTS

Baseline Case Results

Table 2-1 shows the results of VLE calculations for the baseline case as defined in Chapter 1 (495 K, 4.5 MPa), for all three of the vapor fugacity calculation methods considered in this work. While the quantity of direct interest in this project is the vapor-phase mole fraction of water, all compositions in both phases are shown for completeness.

The rigorous calculation from virial coefficients produces a vapor mole fraction of water of 0.5731, much larger than would be obtained from an ideal-gas calculation. Perhaps surprisingly, use of the Peng-Robinson equation for vapor fugacities produces results in fairly good agreement with the more rigorous calculation.

Table 2-1
Equilibrium Liquid (x_i) and Vapor (y_i) Mole Fractions Calculated for the Baseline Case, with Vapor Fugacities Computed by the Ideal-Gas (IG), Virial (Vir), and Peng-Robinson (PR) Methods

i	x_i(IG)	x_i(Vir)	x_i(PR)	y_i(IG)	y_i(Vir)	y_i(PR)
H_2O	0.9986	0.9988	0.9989	0.4817	0.5731	0.5666
Ar	6.87×10^{-6}	6.15×10^{-6}	5.96×10^{-6}	0.0052	0.0043	0.0043
H_2	2.98×10^{-4}	2.72×10^{-4}	2.68×10^{-4}	0.2026	0.1668	0.1693
N_2	4.89×10^{-6}	4.38×10^{-6}	4.32×10^{-6}	0.0052	0.0043	0.0043
CO	2.87×10^{-4}	2.56×10^{-4}	2.53×10^{-4}	0.2131	0.1754	0.1780
CO_2	7.58×10^{-4}	6.32×10^{-4}	6.14×10^{-4}	0.0922	0.0762	0.0774

Effects of Temperature and Pressure

To assess the effect of temperature and pressure on the results, calculations were performed both over a range of temperatures (480 K to 510 K, fixing the pressure at its baseline value of 4.5 MPa), and over a range of pressures (4.0 MPa to 5.0 MPa, fixing the temperature at its baseline value of 495 K). The results of these calculations are shown in Figures 2-1 and 2-2.

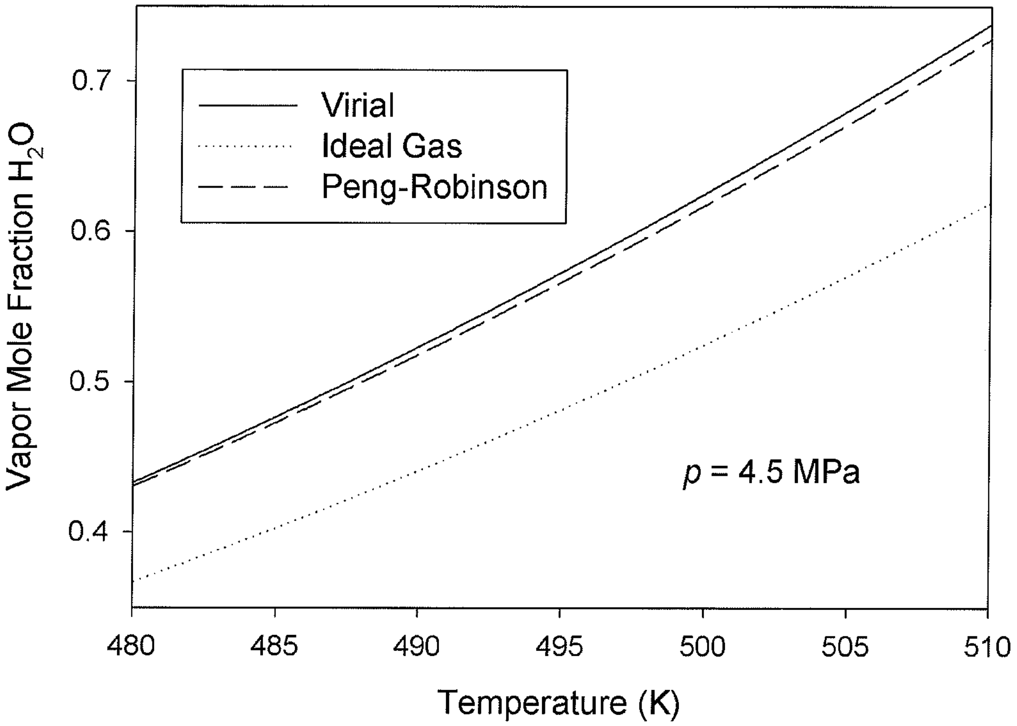

Figure 2-1
Effect of Temperature on Equilibrium Mole Fraction of Water in Vapor at 4.5 MPa

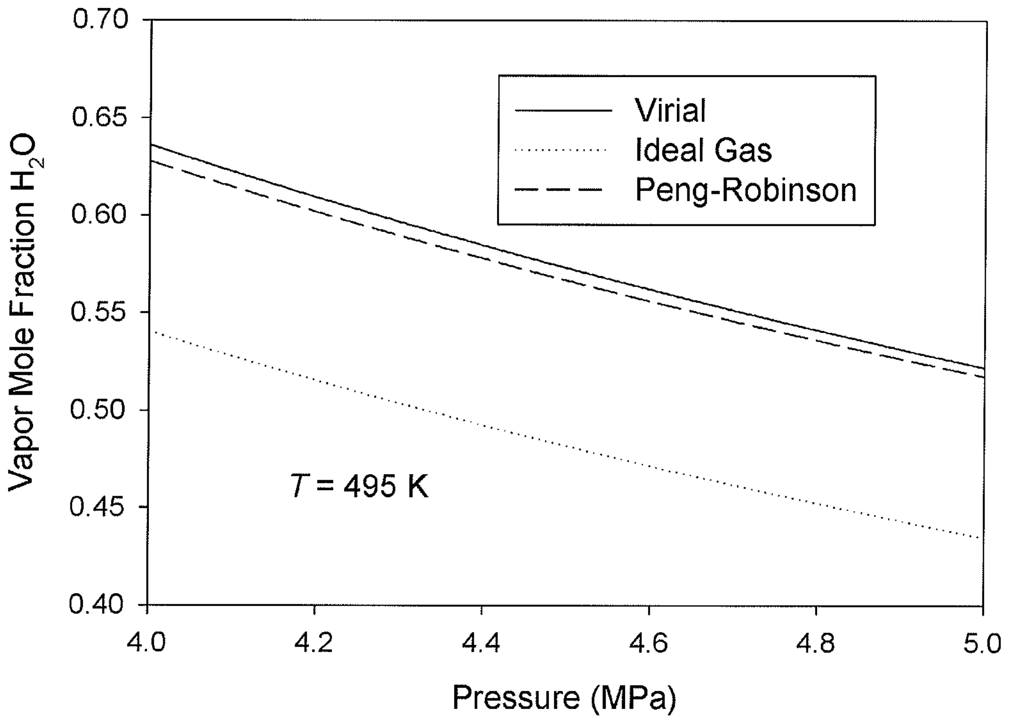

Figure 2-2
Effect of Pressure on Equilibrium Mole Fraction of Water in Vapor at 495 K

Figure 2-1 shows that, as would be expected (because of the increase of the vapor pressure of water with temperature), increasing the temperature at constant pressure results in more water in the vapor phase. The difference between the virial result and the other two vapor fugacity methods grows slowly with temperature, but over the entire range shown the ideal-gas results are seriously in error, while the Peng-Robinson results are reasonable.

Figure 2-2 (note that the scale is different from that in Figure 2-1) shows that an increase in pressure at constant temperature results in a reduced mole fraction of water in the vapor. This also makes physical sense; the partial pressure of water is determined primarily by its vapor pressure as a function of temperature, so any increase in pressure must come from increasing the amount of other components in the synthesis gas. Over this range of pressures at fixed temperature, the relative differences among the three vapor fugacity methods is nearly constant.

Estimation of Uncertainties

Three main sources of uncertainty in the calculated vapor-phase water content can be identified in our model. In the discussion below, we will use the term "uncertainty" to refer to an expanded uncertainty with coverage factor k=2, which approximately corresponds to a 95 % confidence interval.

Uncertainty from Liquid Fugacity Model

The liquid-phase fugacity model introduces only negligible uncertainty. The fugacity of pure water, which is the main part of this model that determines the water content in the vapor, is determined mainly by the vapor pressure of water, which has an uncertainty of approximately 0.02 % in this temperature range. [1] A small correction for pressure is on the order of 1 %, and it is determined by the liquid molar volume, which is known to within 0.1 %. [1]

The gas solubility in the liquid phase is determined primarily by the Henry's constants for the different gases in water, which have uncertainties of roughly 5 % in this temperature range. [2] However, because the resulting solubilities are still quite small (see Table 2-1), the only significant effect of this uncertainty on the VLE results is on the mole fractions of the gases in the liquid phase; the water content in the vapor is not significantly affected.

Uncertainty from Second Virial Coefficients

The water-gas and water-water second virial coefficients all have some uncertainty associated with them (see references in Appendix C). We tested the impact of this uncertainty on the results by perturbing each of these virial coefficients (excluding those for the trace gas components argon and nitrogen) by its (k=2) uncertainty and repeating the calculations for the baseline case. The results are shown in Table 2-2. The results in the table show that this contribution to the uncertainty is also relatively small, contributing to the uncertainty of the water vapor mole fraction by about 0.002 for the second virial coefficient of pure water and by less than 0.001 for each of the water-gas coefficients.

Table 2-2
Effect on Water Content in Vapor of Perturbing Second Virial Coefficient Upward by its (*k*=2) Uncertainty

Second Virial Coefficient Perturbed	Water Mole Fraction in Vapor
(Baseline case)	0.5731
H_2O-H_2O	0.5708
H_2-H_2O	0.5729
CO-H_2O	0.5724
CO_2-H_2O	0.5728

There are also uncertainties in the second virial coefficients not involving water, but their influence on the water content of the vapor is relatively negligible.

Uncertainty from Higher Virial Coefficients

The truncation of the virial expansion after the first correction necessarily introduces some error due to the omission of higher-order terms. These errors will increase with increasing density. We can estimate the effect of higher-order terms by considering the binary system H_2O-CO_2. For this system, experimental values of third virial coefficients in the temperature range of interest are available for pure water, pure CO_2, and for the binary interactions. [1,3,4] These values have large uncertainties, but they serve the purpose of estimating the magnitude of the uncertainty due to virial coefficients beyond the second.

We establish a “baseline” case for the H_2O-CO_2 mixture at the same T and p as our main case. For this case, calculation with our second-virial model yields a water vapor mole fraction of 0.5788. Repeating the calculation with the inclusion of third virial coefficients produces a vapor mole fraction of 0.5857. Further analysis reveals that almost all of this change is due to the third virial coefficient of pure water.

We therefore conclude that the omission of higher virial coefficients causes the vapor mole fraction of water to be underestimated by an amount on the order of 0.005 to 0.01. This is the largest contribution to the uncertainty in our calculation. The fact that most of this deviation appears to be due to the third virial coefficient of pure water suggests that including only that coefficient could reduce this source of uncertainty. However, the improvement in uncertainty would be limited by the large uncertainty in water’s third virial coefficient; two sources for this coefficient differ from each other by about 25 %. [1,5]

Effect of Gas Composition

Some calculations were performed to assess the effect of different gas compositions on the equilibrium water content of the vapor. This was done for each of the major components of the synthesis gas by adding 0.01 to its mole fraction, and reducing the other major components proportionately. The resulting effects were quite small. Increasing the H_2 mole fraction in the synthesis gas by 0.01 changed the water equilibrium mole fraction by –0.00005. Similar increments for CO and CO_2 produced changes of –0.00001 and +0.00009, respectively. So, we can say that the water content in the vapor is enhanced if there is more CO_2 in the synthesis gas and reduced if there is more H_2 in the synthesis gas, but these effects are quite small.

Liquid-Phase Composition

While the water content of the equilibrated vapor is the main quantity of interest in this study, it is worthwhile to make a few observations about the content of the liquid phase. The calculated values for the different gas solubilities at the baseline conditions are shown in Table 2-1. Because CO_2 is more soluble in water than most gases, its mole fraction in the equilibrium liquid is larger than those of the other gases combined, despite its being only 18 % of the synthesis gas. This CO_2 solubility may be important if basic components such as NH_3 are present.

Because the same liquid-phase fugacity model was used in all calculations, the differing liquid compositions shown in Table 2-1 are attributable entirely to the effect on the equilibrium of the vapor fugacity models. In particular, the ideal-gas model overestimates the amount of gas in the liquid phase, because it overestimates the equilibrium mole fractions of the synthesis gases in the vapor phase.

Liquid-phase compositions may be much less accurate if a different liquid fugacity model is used. A few sample calculations were performed where the Peng-Robinson equation was used not only for the vapor fugacities, but also for the liquid fugacities. This option might be more easily available in, for example, process simulation packages. While the vapor-phase compositions from these calculations were still quite accurate, the mole fractions of the gases in the liquid phase were significantly in error, by up to a factor of two in some cases. However, if the liquid-phase mole fractions are of no interest, such an approach could be reasonable.

3
DISCUSSION

Main Results

Calculations were performed of the vapor-liquid equilibrium between water and a typical synthesis gas at conditions of temperature and pressure appropriate for a "quench" of the gas. For the liquid phase, these calculations used the best available data for Henry's constants of gases in water and related quantities. For the vapor phase, they used the thermodynamically rigorous virial expansion truncated at the level of the second virial coefficient. When all uncertainties are considered, the equilibrium mole fraction of water in the vapor phase can be considered accurate to within 0.01, with the largest contribution to the uncertainty coming from the neglect of higher-order virial coefficients.

Other methods of computing the vapor-phase fugacity were examined. The ideal-gas assumption seriously underestimates the water content in the vapor. The Peng-Robinson equation produces only a slight underestimation, similar in size to the uncertainty of the more rigorous calculation. It therefore could be a reasonable option for engineering calculations for this system, at least if the form of the Peng-Robinson equation used is that documented in Appendix C (in particular, the water-specific $a(T)$ term, Eq. (C25), is important). Preferably, the use of the Peng-Robinson equation in this context would only be for the vapor phase, with Henry's law being used for the liquid phase. If the Peng-Robinson equation were used for both phases, the solubilities of gas components in the liquid would not be accurately represented.

The effects of temperature and pressure on the water content of the vapor are as expected; an increase of temperature increases the water content, while an increase of pressure reduces it. The effect of gas composition on the equilibrium water content is very small.

Note on "Adiabatic" Flash Calculations

While the scope of this project was limited to flash calculations at fixed temperature and pressure, a closer approximation to the real industrial situation would be what is commonly known as an "adiabatic" flash calculation, in which the inlet vapor and liquid streams are brought together at a fixed pressure and the outlet temperature and vapor and liquid compositions are determined under the constraint of constant enthalpy. While rigorous adiabatic flash calculations would be a major additional effort beyond the scope of this work, we can offer some qualitative guidance regarding how the results of this work would translate into such a situation.

Because the solubility of the synthesis gas in water is small, the enthalpy balance will be dominated by the vaporization of the water. More vaporization will result in more evaporative cooling; this will be attenuated somewhat by the lower vapor pressure of the water as the temperature decreases. For a given ratio of quench water to synthesis gas, methods that underestimate the equilibrium water content of the vapor at a fixed temperature and pressure (such as the ideal-gas assumption) will overestimate the outlet temperature from the quench step in an adiabatic situation.

Possible Enhancements

Finally, we consider some possibilities for enhancement in the current calculations. These are considered in two categories. The first category involves improvements in the accuracy of the calculations described here. The second category involves enhancements in the scope of the calculations to encompass additional aspects not considered here.

In the first category, as mentioned in Chapter 2, the primary source of uncertainty is the omission of higher-order terms, particularly the third virial coefficient of pure water. Including these higher-order contributions could potentially reduce the uncertainty of the calculated vapor water content by approximately a factor of two. The most important task for such an enhancement would be a critical evaluation of the third virial coefficient of water, in order to estimate its best value and it uncertainty. Uncertainties could also be reduced to a lesser extent by improvements in the theoretical results for the water-gas second virial coefficients; in particular, the H_2O/CO and H_2O/CO_2 interactions are not known as accurately as one might hope.

In the second category, implementing “adiabatic” calculations as described in the previous section is feasible, but would entail significant additional effort to superimpose an enthalpy balance on the VLE calculations. The inclusion of additional trace components in the synthesis gas, beyond those listed in Table 1-1, could also be considered. Sufficient data exist to add O_2 and CH_4; parameters for these gases are listed in Appendices B and C. A significant trace component is H_2S. Sufficient data exist to incorporate H_2S in the liquid-phase fugacity model, but the H_2O/H_2S interaction for the vapor-phase virial model is not known. With regard to potential effects of these trace components, it can be noted that, as pointed out in Chapter 2, the water content of the equilibrium vapor is not very sensitive to small changes in the synthesis gas composition.

Finally, there is a significant complication introduced by the presence of NH_3 in the synthesis gas. NH_3 dissolved in the liquid phase would undergo acid-base reactions with dissolved CO_2 and H_2S; these reactions would significantly enhance the solubilities of these gases. As a result, the present approach would significantly underestimate the amount of NH_3 in the equilibrium liquid, and the solubility of the acid gases would also be somewhat underestimated. However, as long as the NH_3 content in the synthesis gas was small, the effect on the equilibrium water content of the vapor (the main quantity of interest in this work) would be small. In principle it would be possible to incorporate liquid-phase acid-base reactions into the model, but it would be a major effort.

A

VAPOR-LIQUID FLASH CALCULATIONS

Definition of Problem

The calculation defined for the project is the classic "flash" problem, discussed in many textbooks on chemical engineering thermodynamics [6,7].

The known inputs are temperature T, pressure p, and overall composition (in this case, specified flows of water in one input stream and synthesis gas of specified composition in another input stream). The output variables are the mole fractions of each component at equilibrium in both the vapor and liquid phases, and the fraction of the total feed in each phase. The following equations must be solved under the constraint that both phases are at T and p:

$$f_i^{\mathrm{vap}} = f_i^{\mathrm{liq}} \qquad \text{(for each component } i\text{)} \qquad \text{(A1)}$$

$$z_i = \alpha x_i + (1-\alpha) y_i \qquad \text{(for each component } i\text{),} \qquad \text{(A2)}$$

where f_i is the fugacity of component i (which is a function of T, p, and composition), z_i, y_i, and x_i are the mole fraction in the total feed, the equilibrium vapor, and the equilibrium liquid, and □ is the fraction (by mole) of the total feed in the liquid phase at equilibrium. Equation (A1) is the condition of chemical equilibrium between the phases, while Eq. (A2) represents conservation of mass for each component.

For phase-equilibrium calculations, it can be more convenient to work with the fugacity coefficient, defined by $\phi_i = f_i/(x_i p)$. Equation (A1) then becomes

$$\frac{\phi_i^{\mathrm{liq}}}{\phi_i^{\mathrm{vap}}} = \frac{y_i}{x_i} = K_i \qquad \text{(for each component } i\text{),} \qquad \text{(A3)}$$

where the so-called "K-factor" K_i is a key parameter in the flash algorithm.

Description of Algorithm

Many algorithms have been proposed for solving the "flash" problem; for systems such as this where the phases are very dissimilar, a simple algorithm can be used, consisting of the following steps:

1. Assume an equilibrium composition for each phase. In this case, we initially assume that the liquid phase is pure water, while the vapor phase is the composition of the synthesis gas.
2. With this assumed composition, compute the fugacity coefficients ϕ_i^{liq} and ϕ_i^{vap} for each component in each phase, yielding K_i for each component (see Eq. A3).
3. Perform an "ideal flash," solving Eqs. (A2) and (A3) with the values of K_i fixed at their values determined in Step 2. This is a simple matter of finding a value for □ that satisfies the material balance constraint (A2) and the constraints that $\sum_i x_i = 1$ and $\sum_i y_i = 1$. We use an ideal flash algorithm originally programmed by Topliss [8].
4. If the compositions computed in Step 3 have not changed (within some tolerance), the calculation has converged. Otherwise, store the new vapor and liquid compositions determined in Step 3, and go back to Step 2.

In the systems considered here, this algorithm typically converges within about five iterations. We note that, due to the model adopted here for liquid fugacities (see Appendix B), ϕ_i^{liq} is always independent of composition, so it only needs to be computed the first time in Step 2. For calculations where an ideal-gas model is assumed for the vapor, ϕ_i^{vap} is also independent of composition (because it is always 1 for all species), so the initial ideal flash produces the final answer.

B

LIQUID-PHASE FUGACITY MODEL

Fugacity of Gaseous Solutes

The fundamental thermodynamic quantity describing the solubility of a gas in a liquid is the Henry's constant k_H, defined by

$$k_\mathrm{H} = \lim_{x_i \to 0} \left(f_i / x_i \right), \tag{B1}$$

where f_i and x_i are, respectively, the liquid-phase fugacity and mole fraction of the solute i. While this definition can be applied at any state of the solvent, in this work we restrict our attention to vapor-liquid equilibrium conditions in single solvents, so that k_H is a function only of temperature along the vapor-liquid saturation curve of the solvent.

At small solute gas pressures, Eq. (B1), with the limit removed, would be sufficient to relate the solute fugacities to the mole fraction. However, there is a (small but not negligible) thermodynamic correction for higher pressures, giving the result: [6]

$$\ln\left(f_i / x_i \right) = \ln k_\mathrm{H} + \frac{\bar{v}_i^\infty \left(p - p^\mathrm{s} \right)}{RT}, \tag{B2}$$

where $\bar{v}_i^\infty$ is the infinite-dilution partial molar volume of solute i in the solvent, p is the pressure, p^s is the saturation vapor pressure of the solvent, R is the molar gas constant, and T is the absolute temperature. If the pressure is equal to the solvent vapor pressure p^s, the correction term becomes zero and Eq. (B1) is recovered.

For phase-equilibrium calculations as implemented in this work, what is required is not the fugacity f_i but the fugacity coefficient $\phi_i = f_i / (x_i p)$. Manipulation of Eq. (B2) produces the following expression for the solute fugacity coefficient ϕ_i:

$$\phi_i = \frac{k_\mathrm{H} \exp\left(\dfrac{\bar{v}_i^\infty \left(p - p^\mathrm{s} \right)}{RT} \right)}{p}. \tag{B3}$$

The most important factor in Eq. (B3) is the Henry's constant k_H. We use values from the critical data evaluation of Fernández-Prini et al., who correlated their results for each solute as a function of temperature with a theory-based expression: [2]

$$\ln\left(k_H / p^s\right) = A / T_R + \frac{B\tau^{0.355}}{T_R} + C(T_R)^{-0.41} \exp\tau, \tag{B4}$$

where $\tau = 1 - T_R$, $T_R = T / T_c$, and T_c is the critical temperature of the solvent (647.096 K for H_2O). Table B-1 contains the parameters A, B, and C for each solute in water, along with the minimum and maximum temperatures of correlation.

Table B-1
Parameters for Eq. (B4), along with Maximum and Minimum Temperatures of Data Used for the Correlation [2]

Solute	*A*	*B*	*C*	T_{min} (K)	T_{max} (K)
Ar	-8.40954	4.29587	10.52779	273.19	568.36
H_2	-4.73284	6.08954	6.06066	273.15	636.09
N_2	-9.67578	4.72162	11.70585	278.12	636.46
O_2	-9.44833	4.43822	11.42005	274.15	616.52
CO	–10.52862	5.13259	12.01421	278.15	588.67
CO_2	-8.55445	4.01195	9.52345	274.19	642.66
CH_4	–10.44708	4.66491	12.12986	275.46	633.11

Both Eqs. (B3) and (B4) require p^s, the vapor pressure of water at the temperature of interest. This is calculated from the international standard correlation of Wagner and Pruss, which has the following functional form:

$$\ln\left(p^s / p_c\right) = (T_c / T)\left(a_1\tau + a_2\tau^{1.5} + a_3\tau^3 + a_4\tau^{3.5} + a_5\tau^4 + a_6\tau^{7.5}\right), \tag{B5}$$

where p_c is water's critical pressure (22.064 MPa), and τ and T_c are defined below Eq. (B3). The values of the coefficients are $a_1 = -7.85951783$, $a_2 = 1.84408259$, $a_3 = -11.7866497$,
$a_4 = 22.6807411$, $a_5 = -15.9618719$, $a_6 = 1.80122502$. [9]

The final quantity required for computation of the solute fugacity coefficients by Eq. (B3) is the solute partial molar volume $\bar{v}_i^\infty$ at infinite dilution in water. This quantity is calculated as described by Fernández-Prini and Japas based on a molecular perturbation theory. [10,11] Their final expression is

$$\bar{v}_i^\infty = RT\chi_T\left\{1 + \frac{\eta}{1-\eta}\left[1 + 3\frac{r+r^2}{1-\eta} + 9\frac{\eta r^2}{(1-\eta)^2} + \frac{(1+2\eta)^2}{(1-\eta)^3}r^3\right]\right\}, \tag{B6}$$

where □ is the "packing fraction" of the pure solvent (water), defined by $\eta = \pi N_A \rho_w d_w^3 / 6$, where ρ_w is the molar density of water, d_w is the characteristic diameter of a water molecule (taken as 0.27 nm in all cases here), and N_A is Avogadro's number. r is the ratio d_i/d_w, where d_i is a characteristic diameter for the solute molecule. $□_T$ is the isothermal compressibility of pure water.

The pure-water properties ρ_w and $□_T$ are obtained from the NIST Standard Reference Database for water properties. [12] The only parameter required for the calculation of $\bar{v}_i^\infty$ is then d_i, which is correlated as a function of temperature by one of two functional forms: [11]

$$d_i = d_i^\circ + b_i(T - 298\,\mathrm{K}), \tag{B7a}$$

$$d_i = d_i^\circ + b_i' \ln(T / 298\,\mathrm{K}). \tag{B7b}$$

Table B-2 contains the parameters d_i° and b_i or b_i' for all the solutes considered in this work.

Table B-2
Parameters for Eq. (B7) (last column is b_i for all solutes except CO_2, where it is b_i') [11].

Solute	d_i° **(nm)**	b_i (nm/K) or b_i' (nm)
Ar	0.241	-2.01×10^{-4}
H_2	0.266	-1.25×10^{-4}
N_2	0.339	-1.70×10^{-4}
O_2	0.342	-2.00×10^{-4}
CO	0.353	-2.53×10^{-4}
CO_2	0.427	-0.2246
CH_4	0.369	-3.05×10^{-4}

We note that, at the pressures and temperatures of interest in this work, the correction to the solute fugacity coefficients provided by the $\bar{v}_i^\infty$ term is typically on the order of one or two percent. Its accuracy is therefore not crucial in the context of the present project.

Fugacity of Liquid Water

Under the conditions considered here (dilute solution of solute gases), the calculation of the fugacity of liquid water is straightforward, given merely by its fugacity in the pure state f_w^{pure} at the temperature and pressure of interest (obtained from [12]) multiplied by its mole fraction (which is slightly less than 1 due to the solubility of the solute gases). The equation for the fugacity coefficient becomes

$$\phi_{\mathrm{w}} = \frac{f_{\mathrm{w}}^{\mathrm{pure}}\left(1-\sum_i x_i\right)}{x_{\mathrm{w}}p} = \frac{f_{\mathrm{w}}^{\mathrm{pure}}}{p}. \qquad \text{(B8)}$$

Impact on Calculations

It can be noted that the main quantity of interest in this project (the amount of water in the equilibrium vapor phase) is not very sensitive to the liquid-phase fugacity calculations (other than the calculation of $f_{\mathrm{w}}^{\mathrm{pure}}$, which is well-known). The solute fugacity coefficients as calculated in Eq. (B3) primarily influence the solubility of the gases x_i. While these solubilities may be of interest for some applications, they are small enough that their impact on the equilibrium fugacity of water is generally less than 1 %.

We also note that, due to the structure of the model, both the solute fugacity coefficients ϕ_i (Eq. B3) and the water fugacity coefficient ϕ_{w} (Eq. B8) depend only on temperature and pressure, but not on the liquid-phase composition. This simplifies the vapor-liquid equilibrium calculations, as discussed in Appendix A.

C
VAPOR-PHASE FUGACITY MODEL

Calculation from Virial Coefficients

For gas-phase systems, a rigorous description of the thermodynamics is provided by the virial expansion, which is written as a series of corrections to the ideal-gas law:

$$\frac{p}{\rho RT} \equiv z = 1 + B\rho + C\rho^2 + \ldots, \tag{C1}$$

where p is the pressure, ρ the molar density, R the molar gas constant, and T the absolute temperature. The quotient z (which is 1 for an ideal gas) is usually called the *compressibility factor*, B is called the *second virial coefficient*, C the *third virial coefficient*, and so forth. An alternative form of the expansion can be formulated as a power series in p rather than ρ, but it has been shown that the pressure form is generally less accurate than the density form when truncated at the same level. [13]

For mixtures, the virial coefficients are rigorously given as mole-fraction-weighted sums over characteristic binary quantities (for B), ternary quantities (for C), etc. For B, the expression is

$$B_{\text{mix}}(T) = \sum_i \sum_j y_i y_j B_{ij}(T), \tag{C2}$$

where y is the mole fraction of the species in the vapor mixture and the sums extend over all components. B_{ij} is completely determined by the interactions between one molecule of species i and one of species j. For a given pair, it is a function of temperature only. If i=j, $B_{ij}(T)$ is just the pure-component value of $B(T)$; these values are well known for the substances of interest here. Obtaining reliable values of $B_{ij}(T)$ for unlike pairs is more difficult, and has been the main focus of this project.

At moderate pressures, it is adequate to truncate Eq. (C1) after the term involving the second virial coefficient. Standard thermodynamic manipulations then produce the following expression for the fugacity coefficient for each species: [6]

$$\ln \phi_i = 2\rho \sum_j y_j B_{ij} - \ln z, \tag{C3}$$

where the sum is over all species including i. The molar density ρ (and therefore the compressibility factor z) is solved for iteratively from Eq. (C1) once all the virial coefficients are known. Use of Eq. (C3) requires knowledge of all the second virial coefficients $B_{ij}(T)$ for all pairs of species in the system.

B(T) Data for Pure Components

$B(T)$ for pure water is taken from the correlation of Harvey and Lemmon, which has the form

$$B(T)/B^0 = a_1(T^*)^{-0.5} + a_2(T^*)^{-0.8} + a_3(T^*)^{-3.35} + a_4(T^*)^{-8.3}, \qquad \text{(C4)}$$

where $B^0 = 1000$ cm^3/mol, $T^* = T/100$ K, $a_1 = 0.34404$, $a_2 = -0.75826$, $a_3 = -24.219$, and $a_4 = -3978.2$. [14]

$B(T)$ for pure oxygen is taken the work of from Wagner et al.:

$$B(T)/B^0 = b_1 + b_2(T^*)^{-0.25} + b_3(T^*)^{-3.5} + b_4(T^*)^{-4.5} + b_5(T^*)^{-5.5}, \qquad \text{(C5)}$$

where $B^0 = 1000$ cm^3/mol, $T^* = T/1$ K, $b_1 = 0.143389$, $b_2 = -0.629863$, $b_3 = -0.577814 \times 10^7$, $b_4 = 0.695858 \times 10^9$, and $b_5 = -0.246023 \times 10^{11}$. [15]

$B(T)$ for pure hydrogen is taken from a correlation by Hodges et al.:

$$B(T)/B^0 = a_1(T^*)^{-0.33} + a_2(T^*)^{-1.4} + a_3(T^*)^{-1.8} + a_4(T^*)^{-2.2}, \qquad \text{(C6)}$$

where $B^0 = 1$ cm^3/mol, $T^* = T/100$ K, $a_1 = 42.0803$, $a_2 = -143.982$, $a_3 = 146.918$, and $a_4 = -47.5601$. [16]

For other pure species, $B(T)$ is taken from the reference-quality equations of state implemented in the NIST Refprop database. [3] The expressions for $B(T)$ derived from these equations take the form:

$$B(T)/\rho_c = \sum_i a_i \tau^{b_i}, \qquad \text{(C7)}$$

where ρ_c is the critical density of the fluid, $\tau = T_c/T$, where T_c is the critical temperature of the fluid, and the a_i and b_i are a series of parameters specific to the fluid. Table C-1 gives parameters a_i and b_i for use in Eq. (C7), and Table C-2 lists the values of the critical constants.

Table C-1
Parameters for Eq. (C4) for $B(T)$ of Ar, N_2, CO, CO_2, and CH_4

Param.	Ar	N_2	CO	CO_2	CH_4
a_1	0.08872230499	0.924803575275	0.90554	0.388568232032	0.04367901028
a_2	0.705148051673	-0.492448489428	-2.4515	2.93854759427	0.6709236199
a_3	-1.68201156541	0.564857472498	0.53149	-5.58671885349	-1.765577859
a_4	-0.149090144315	-1.61720005987	-0.12778	-0.767531995925	0.1830487909
a_5	-0.120248046009	-0.481395031883	*(not used)*	2.16589615432	0.1511883679
a_6	-0.321813917507	-0.0435762336045	*(not used)*	-0.370556852701	-0.4289363877
a_7	0.332300176958	*(not used)*	*(not used)*	-0.0167758797004	-0.01932040831
b_1	0	0.25	0.25	0	-0.5
b_2	0.25	0.875	1.125	0.75	0.5
b_3	1	0.5	1.5	1	1
b_4	2.75	0.75	3.625	2	0
b_5	4	2	*(not used)*	1.5	1
b_6	3	4	*(not used)*	3	2
b_7	3.5	*(not used)*	*(not used)*	6	5

Table C-2
Critical Parameters and Acentric Factor for Substances Considered in this Work

Substance	T_c (K)	p_c (kPa)	ρ_c (mol/dm^3)	ω
H_2O	647.096	22064.	17.873728	0.3443
Ar	150.687	4863.	13.4074	-0.00219
H_2	33.145	1296.4	15.508	-0.219
N_2	126.192	3395.8	11.1839	0.0372
O_2	154.581	5043.	13.63	0.0222
CO	132.86	3494.	10.85	0.0497
CO_2	304.1282	7377.3	10.6249	0.22394
CH_4	190.564	4599.2	10.139	0.01142

B(T) Data for Aqueous Binaries

The $B_{ij}(T)$ for pairs where water is one of the components are the most important factors determining the vapor-phase fugacity coefficient in Eq. (C3), and therefore are the most important in determining the equilibrium mole fraction of water in the vapor. For the most part, these are obtained from a series of recently published works making use of quantum chemistry. [16,17,18,19,20,21] The exception is the H_2O/CO_2 system, where the experimental data of Patel et al. cover the temperature range of interest and were fitted for this work to a simple functional form. [4]

The equations for $B_{ij}(T)$ for most of these pairs take a form similar to that of Eq. (C4):

$$B_{ij}(T)/B^0 = a_1(T^*)^{b_1} + a_2(T^*)^{b_2} + a_3(T^*)^{b_3} + a_4(T^*)^{b_4}, \tag{C8}$$

where $B^0 = 1000\ \text{cm}^3/\text{mol}$ and $T^* = T/100\ \text{K}$. Values of the a and b coefficients for each aqueous binary for use in Eq. (C8) are given in Table C-3. Information about the uncertainty of these correlations may be found in the original references.

Table C-3
Parameters for Eq. (C8) for $B_{ij}(T)$ for H_2O with Various Gases

Parameter	H_2O/Ar [17]	H_2O/H_2 [16]	H_2O/N_2 [19]	H_2O/O_2 [20]	H_2O/CO [21]	H_2O/CO_2 [4]
a_1	96.1941	33.047	67.595	124.605	485.062	–3308.1
a_2	–211.074	–250.41	–249.83	–214.421	–2054.24	*(not used)*
a_3	–96.4425	285.42	–204.38	–102.818	7422.08	*(not used)*
a_4	–12.6006	–186.78	*(not used)*	–22.360	–5919.89	*(not used)*
b_1	–0.31	–0.21	–0.24	–0.33	–0.18	–2.66
b_2	–0.82	–1.50	–1.06	–0.73	–1.70	*(not used)*
b_3	–2.24	–2.26	–3.22	–2.03	–2.10	*(not used)*
b_4	–4.60	–3.21	*(not used)*	–4.07	–2.25	*(not used)*

The only aqueous binary for which $B_{ij}(T)$ is not described by Eq. (C8) is H_2O/CH_4, for which the correlation is

$$B_{ij}(T)/(1\ \text{cm}^3/\text{mol}) = \sum_{i=1}^{6} a_i (T_0/T)^i, \tag{C9}$$

where $T_0 = 599.216$ K, $a_1 = 109.447$, $a_2 = -227.694$, $a_3 = 182.497$, $a_4 = -80.944$, $a_5 = 18.368$, and $a_6 = -1.673$. [18]

B(T) Data for Nonaqueous Binaries

The $B_{ij}(T)$ for pairs where neither component is water play a minor but not negligible role in the phase equilibrium. For these binaries, we make use of a corresponding-states correlation developed by Tsonopoulos. [22] The correlation takes the form

$$\frac{B(T)p_c}{RT_c} = F^{(0)}\left(\frac{T}{T_c}\right) + \omega F^{(1)}\left(\frac{T}{T_c}\right), \tag{C10}$$

with

$$F^{(0)}\left(\frac{T}{T_c}\right) = 0.1455 - \frac{0.330}{T_R} - \frac{0.1385}{T_R^2} - \frac{0.0121}{T_R^3} - \frac{0.000607}{T_R^8}, \tag{C11}$$

$$F^{(1)}\left(\frac{T}{T_c}\right) = 0.0637 + \frac{0.331}{T_R^2} - \frac{0.423}{T_R^3} - \frac{0.008}{T_R^8}. \tag{C12}$$

p_c and T_c are the critical pressure and temperature, respectively. ω is the acentric factor, a semi-theoretical parameter related to the degree to which a substance deviates from a "simple" fluid; values for ω are well-known for most common fluids. T_R is the reduced temperature, $T_R = T/T_c$. Critical properties and acentric factors for all fluids used in this work are taken from the NIST Refprop database [3] and are listed in Table C-2.

For "quantum" gases (those such as H_2 with such low molecular masses that their thermodynamic properties are affected by quantum mechanics), temperature-dependent "effective" critical constants are used, defined as follows:

$$T_c = \frac{T_c^0}{1 + \frac{21.8}{MT}}, \tag{C13}$$

$$p_c = \frac{p_c^0}{1 + \frac{44.2}{MT}}. \tag{C14}$$

T_c^0 and p_c^0 are hypothetical values that the critical temperature and pressure would have in the absence of quantum effects, and M is the relative molar mass. For H_2, the only quantum fluid considered in this project, $T_c^0 = 43.6$ K, $p_c^0 = 2.05$ MPa, and $M = 2.01594$.

In order to use Eq. (C10) to derive $B_{ij}(T)$ for unlike pairs, combining rules are required to obtain characteristic values of T_c, p_c, ω, and M (if one of the pair is H_2) for use in the Tsonopoulos correlation. As suggested in the literature, the following combining rules are used: [6,22]

$$T_{c,ij} = \left(T_{c,i}T_{c,j}\right)^{1/2}\left(1 - k_{ij}\right), \tag{C15}$$

$$p_{c,ij} = \frac{4T_{c,ij}\left(p_{c,i}v_{c,i}/T_{c,i} + p_{c,j}v_{c,j}/T_{c,j}\right)}{\left(v_{c,i}^{1/3} + v_{c,j}^{1/3}\right)^3}, \tag{C16}$$

$$\omega_{ij} = 0.5(\omega_i + \omega_j), \tag{C17}$$

$$M_{ij}^{-1} = 0.5(M_i^{-1} + M_j^{-1}). \tag{C18}$$

The binary parameter k_{ij} in Eq. (C15) is set to zero in the absence of data, but can be adjusted to fit experimental data if they are available. Table C-4 lists values of k_{ij} (which is the same as k_{ji}) and the corresponding sources of mixture data for a number of binaries in this work. For those not listed in the table, a value of 0 is used.

Table C-4
Binary Parameters k_{ij} for Eq. (C15) for Pairs of Nonaqueous Gases

Component *i*	**Component *j***	k_{ij}	**Data Source**
Ar	H_2	–0.12	[23]
Ar	N_2	–0.01	[23]
Ar	O_2	0.00	[23]
Ar	CO	–0.01	[24]
Ar	CO_2	0.05	[23]
Ar	CH_4	0.02	[23]
H_2	N_2	–0.04	[24]
H_2	CO	–0.04	[24]
H_2	CO_2	–0.04	[25]
H_2	CH_4	–0.05	[24]
N_2	O_2	–0.01	[23]
N_2	CO	–0.02	[26]
N_2	CO_2	–0.01	[23,27]
N_2	CH_4	0.03	[23,28]
O_2	CO_2	0.05	[23]
O_2	CH_4	0.04	[23]
CO	CO_2	–0.04	[29]
CO	CH_4	0.01	[24]
CO_2	CH_4	0.05	[23,27]

Supplementary Calculation with Peng-Robinson Equation of State

For comparison purposes, some calculations for this project were performed with the semiempirical Peng-Robinson equation of state. [30,31] The Peng-Robinson equation has the following form:

$$p = \frac{RT}{v-b} - \frac{a(T)}{v(v+b)+b(v-b)}, \tag{C19}$$

where p is the pressure, T is the absolute temperature, v is the molar volume, and R is the molar gas constant. a and b are substance-specific parameters; b is a constant depending only on the critical properties, while a is a function of temperature in a manner that depends on the acentric factor ω:

$$b = 0.778\frac{RT_\mathrm{c}}{p_\mathrm{c}}, \tag{C20}$$

$$a(T) = a(T_\mathrm{c})\alpha(T), \tag{C21}$$

$$a(T_\mathrm{c}) = 0.45724\frac{(RT_\mathrm{c})^2}{p_\mathrm{c}}, \tag{C22}$$

$$\alpha(T) = \left[1+\beta\left(1-\sqrt{T/T_\mathrm{c}}\right)\right]^2, \tag{C23}$$

$$\beta = 0.37464 + 1.54226\omega - 0.26992\omega^2. \tag{C24}$$

We make use of a special parameterization introduced by Peng and Robinson for $a(T)$ for water: [31]

$$a_\mathrm{w}(T) = \left[1.0085677 + 0.82154\left(1-\sqrt{T/T_\mathrm{c}}\right)\right]^2, \text{ for } \sqrt{T/T_\mathrm{c}} < 0.85. \tag{C25}$$

When $\sqrt{T/T_\mathrm{c}} \geq 0.85$, Eqs. (C23-C24) are used as with other fluids.

Use of the Peng-Robinson equation for mixtures requires mixing rules for the parameters a and b based on their pure component values:

$$a = \sum_i \sum_j y_i y_j a_{ij}, \tag{C26}$$

$$b = \sum_i y_i b_i, \tag{C27}$$

where y_i is the mole fraction of component i. For unlike pairs, a combining rule is needed for a_{ij} based on pure-component values a_i and a_j:

$$a_{ij} = \left(a_i a_j\right)^{1/2}. \tag{C28}$$

It is possible to introduce an adjustable binary parameter into Eq. (C28) (similar to that in Eq. (C15)) in order to attempt to fit experimental data more closely, but that enhancement was not explored in this project.

From the Peng-Robinson equation, the equation for the fugacity coefficient ϕ_i of a component i is: [6]

$$\ln\phi_i = \frac{b_i}{b}\left(\frac{pv}{RT}-1\right) - \ln\frac{p(v-b)}{RT} - \frac{a}{2\sqrt{2}bRT}\left[\frac{2\sum_j y_j a_{ji}}{a} - \frac{b_i}{b}\right]\ln\frac{v+\left(1+\sqrt{2}\right)b}{v+\left(1-\sqrt{2}\right)b}. \tag{C29}$$

The accuracy of our implementation of the Peng-Robinson equation was tested by verifying that calculated results for densities and fugacity coefficients matched those from an independently programmed implementation available in a NIST database. [3]

D
REFERENCES

---

[1] W. Wagner and A. Pruß, *J. Phys. Chem. Ref. Data* **31**, 387 (2002).

[2] R. Fernández-Prini, J.L. Alvarez, and A.H. Harvey, *J. Phys. Chem. Ref. Data* **32**, 903 (2003).

[3] E.W. Lemmon, M.L. Huber, and M.O. McLinden, *REFPROP: Reference Fluid Thermodynamic and Transport Properties*, NIST Standard Reference Database 23, Version 8.0 (National Institute of Standards and Technology, Gaithersburg, MD 2007).

[4] M.R. Patel, J.C. Holste, K.R. Hall, and P.T. Eubank, *Fluid Phase Equil.* **36**, 279 (1987).

[5] P.G. Hill and R.D.C. Macmillan, *Ind. Eng. Chem. Res.* **27**, 874 (1988).

[6] J.M. Prausnitz, R.N. Lichtenthaler, and E. Gomes de Azevedo, *Molecular Thermodynamics of Fluid-Phase Equilibria*, 3rd ed. (Prentice Hall, Upper Saddle River, NJ, 1999).

[7] J.M. Smith and H.C. Van Ness, *Introduction to Chemical Engineering Thermodynamics*, 3rd ed. (McGraw-Hill, New York, 1975).

[8] R.J. Topliss, *Techniques to Facilitate the Use of Equations of State for Complex Fluid-Phase Equilibria* (Dissertation, Univ. of California-Berkeley, 1985).

[9] W. Wagner and A. Pruss, *J. Phys. Chem. Ref. Data* **22**, 783 (1993).

[10] R. Fernández-Prini and M.L. Japas, *J. Phys. Chem.* **93**, 3802 (1989).

[11] R.J. Fernández-Prini, H.R. Corti, and M.L. Japas, *High-Temperature Aqueous Solutions: Thermodynamic Properties* (CRC Press, Boca Raton, FL 1992).

[12] A.H. Harvey, A.P. Peskin, and S.A. Klein, *NIST/ASME Steam Properties*, NIST Standard Reference Database 10, Version 2.21 (National Institute of Standards and Technology, Gaithersburg, MD 2000).

[13] P.T. Eubank, H. Kruggel-Emden, G. Santana-Rodriguez, and X. Wang, *Fluid Phase Equilib.* **207**, 35 (2003).

[14] A.H. Harvey and E.W. Lemmon, *J. Phys. Chem. Ref. Data* **33**, 369 (2004).

[15] W. Wagner, J. Ewers, and R. Schmidt, *Cryogenics* **24**, 37 (1984).

[16] M.P. Hodges, R.J. Wheatley, G.K. Schenter, and A.H. Harvey, *J. Chem. Phys.* **120**, 710 (2004).

[17] M.P. Hodges, R.J. Wheatley, and A.H. Harvey, *J. Chem. Phys.* **117**, 7169 (2002).

[18] O. Akin-Ojo, A.H. Harvey, and K. Szalewicz, *J. Chem. Phys.* **125**, 014314 (2006).

[19] A.S. Tulegenov, R.J. Wheatley, M.P. Hodges, and A.H. Harvey, *J. Chem. Phys.* **126**, 094305 (2007).

[20] R.J. Wheatley and A.H. Harvey, *J. Chem. Phys.* **127**, 074303 (2007).

[21] R.J. Wheatley and A.H. Harvey, *J. Chem. Phys.*, to be submitted (2008). $B_{ij}(T)$ data used for this work are preliminary and subject to change.

[22] C. Tsonopoulos, *AIChE J.* **20**, 263 (1974).

[23] M.J. Martin, R.D. Trengove, K.R. Harris, and P.J. Dunlop, *Aust. J. Chem.* **35**, 1525 (1982).

[24] J. Brewer, *Determination of Mixed Virial Coefficients*, AFOSR 67-2795 (Air Force Office of Scientific Research, Arlington, VA, 1967).

[25] B.D. Ababio and P.J. McElroy, *J. Chem. Thermodyn.* **25**, 1495 (1993).

[26] P.J. McElroy and S. Buchanan, *J. Chem. Thermodyn.* **27**, 755 (1995).

[27] H.B. Brugge, C.-A. Hwang, W.J. Rogers, J.C. Holste, K.R. Hall, W. Lemming, G.J. Esper, K.N. Marsh, and B.E. Gammon, *Physica A* **156**, 382 (1989).

[28] B.D. Ababio, P.J. McElroy, and C.J. Williamson, *J. Chem. Thermodyn.* **33**, 413 (2001).

[29] P.J. McElroy and J. Moser, *J. Chem. Thermodyn.* **27**, 267 (1995).

[30] D.-Y. Peng and D.B. Robinson, *Ind. Eng. Chem. Fundam.* **15**, 59 (1976).

[31] D.-Y. Peng and D.B. Robinson, Ch. 20 in S.A. Newman (ed.), *Thermodynamics of Aqueous Systems with Industrial Applications* (ACS Symposium Series 133, American Chemical Society, Washington, 1980), p. 393.

[32] *Program on Technology Innovation: Thermodynamic Data to Support High-Temperature Syngas Quench Design: Vapor-Liquid Equilibrium Calculations.* EPRI, Palo Alto, CA: 2007. 1015542.